Available online at www.sciencedirect.com

ScienceDirect

Journal of Magnesium and Alloys 9 (2021) 1458–1469

www.elsevier.com/locate/jma

Role of heat balance on the microstructure evolution of cold spray coated AZ31B with AA7075

Bahareh Marzbanrad, Mohammad Hadi Razmpoosh, Ehsan Toyserkani, Hamid Jahed*

Mechanical and Mechatronics Engineering Department, University of Waterloo, Canada

Received 29 September 2020; received in revised form 15 February 2021; accepted 12 March 2021
Available online 9 April 2021

Abstract

A promising solid-state coating mechanism based on the cold spray technique provides highly advantageous conditions on thermal-sensitive magnesium alloys. To study the effect of heat balance in cold spray coating on microstructure, experiments were designed to successfully coat AA7075 on AZ31B with two different heat balance conditions to yield a coated sample with tensile residual stress and a sample with compressive residual stress in both coating and substrate. The effects of coating temperature on the microstructure of magnesium alloy and the interfaces of coated samples were then analyzed by SEM, EBSD, TEM in high- and low-heat input coating conditions. The interface of the AA7075 coating and magnesium alloy substrate under both conditions consists of a narrow-band layer with very fine grains, followed by columnar grains of magnesium that have grown perpendicular to the interface. At higher temperatures, this layer became wider. No intermetallic phase was detected at the interface under either condition. It is shown that the microstructure of the substrate was affected by coating temperature, leading to stress relief, dynamic recrystallization and even dynamic grain growth of magnesium under high temperature. Reducing the heat input and increasing the heat transfer decreased microstructural changes in the substrate.

Keywords: Cold spraying; Heat balance; Microstructural analysis; Coating interface; Magnesium Alloy AZ31B; Residual Stress.

1. Introduction

Motivated by environmental concerns, there is an increasing trend towards lighter-weight vehicle structures in both the automotive and aerospace industries [1]. The lightest commercially available structural metals, magnesium and its alloys, are valued for their high strength-to-weight ratio and low energy consumption during manufacturing processes and are thus of interest to researchers designing lighter vehicles [2]. However, the application of magnesium and its alloys is mainly restricted to non-load-bearing components. Weaknesses such as the poor corrosion resistance [3] and low fatigue strength of magnesium alloys are obstacles in the growing market and are a major barrier to extending their application to load-bearing components. One approach to overcoming the durability drawbacks is to coat the surface of magnesium with a relatively high fatigue strength material [4]. A defect-free coating of a high strength material, AA7075 aluminum alloy, on a magnesium substrate has the potential to boost the mechanical properties and induce beneficial residual stresses. The AA7075 cold spray deposited layer can delay fatigue crack initiations and impede crack propagation in the coating and the substrate due to the higher fatigue strength than magnesium alloy. However, the temperature of the cold spray process can be high enough to change the residual stress and microstructure of magnesium alloys. These changes are resulted from the accumulation of thermal energy from particle impact accompanied by a carrier gas; consequently, tensile residual stresses may be induced in both coating and substrate. Therefore, by controlling the heat balance, the residual stress in the substrate can be tailored to the desirable pattern [5]. However, the effect of the heat balance on the microstructure of the magnesium substrate has not yet been studied.

* Corresponding author.
E-mail addresses: hamid.jahed@uwaterloo.ca, hjahedmo@uwaterloo.ca (H. Jahed).

https://doi.org/10.1016/j.jma.2021.03.009

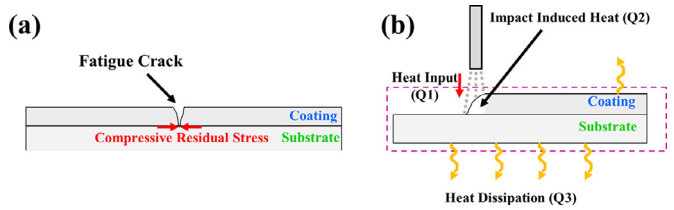

Fig. 1. a) Compressive residual stress at the interface with potentials to delay fatigue crack growth; b) Heat balance of the cold spray coating system.

Cold spray is a versatile technology in which particles are accelerated to a supersonic speed to collide with a surface and create a dense coating layer by local plastic deformation [6,7,8]. Due to the particles' relatively low temperature during the process (lower than their melting point) and because they impact with high kinetic energy, compressive residual stress and grain refinement in the coating and substrate parallel and near to the surface has been reported [9–11]. Thus, crack initiation from the coated surface as well as the interface is delayed, and crack propagation into the substrate is postponed (Fig. 1a) [12]. These desirable conditions can be achieved in magnesium alloys by coating them with a dense layer of high fatigue strength material such as AA7075 [4]. Despite the expectations, the cold spray coating process was found to create tensile residual stress in the magnesium alloy substrate near the interface [13], which can have a detrimental impact on the fatigue life of magnesium parts. Increased temperature of the substrate during coating and thermal mismatch were shown to be responsible for inducing unfavorable residual stress in the substrate [8,11]. On the other hand, the temperature gradient during the deposition and cooling after coating can influence the microstructure of a substrate, especially near the interface. Therefore, the likelihood of microstructural evolutions and residual stress changes such as dynamic recovery, recrystallization, dynamic grain growth, or stress relief needs to be carefully investigated.

To examine microstructural changes and residual stress changes in substrates during coating, the authors have proposed a technique for controlling the heat balance of the system to decrease the target surface's interface temperature [5]. The heat input and output of such a system (highlighted by the dashed line) is summarized in Fig. 1b. In the system, the heat balance occurs between the heat energy input to the system, including heat input from the carrier gas (Q1), heat generation due to the particles' impact (Q2), and heat dissipation to the surroundings (Q3), and especially, through heat conduction to the substrate, which has a higher rate than heat convection or radiation. Increasing the nozzle's travel speed at a constant feed rate decreases the coating time, which in turn lowers Q1. At the same time, it results in less material deposited on the substrate, which reduces Q2. Based on results reported for AA7075-AZ31B coated samples [5,13] increasing the nozzle speed decreases the tensile residual stress, but this was shown to be not enough to change stresses to compressive residual stresses. However, by improving the substrate's heat dissipation Q3 with optimized Q1 and Q2, the substrate residual stress turned into compressive stress [5].

The aim of this research is to investigate the microstructural evolution of the interface and substrate when high and low thermal energy balance coatings are performed, resulting in tensile and compressive residual stress in the substrate. To achieve this, two sets of cold spray parameters are used to develop the tensile and compressive residual stress in the substrate. The respective samples are herein called the tensile and the compressive sample. The residual stresses in the coating and substrate are measured using a hole drilling technique. Then, the crystal structure of the interface is analyzed by the XRD method. SEM, EBSD and TEM techniques have also been employed to evaluate the difference between the microstructure of the substrate and interface for the two types of samples, which have experienced different coating conditions.

2. Experimental procedure

2.1. Materials

Six rectangular pieces of as-received AZ31B-H24 samples (50×30×3.16 mm) were prepared, and then the samples were stress relieved based on the ASM-recommendation procedure (260ºC/15 min) [14]. Spherical-shaped AA7075 powder (supplied by Centerline Ltd., Windsor, Canada) with an average particle size of 23 μm (measured by Retsch technology, Camsizer XT) was deposited on the magnesium alloy samples. The chemical compositions of AA7075 powder are listed in Table 1.

2.2. Coating parameters

A low-pressure cold spray system (SST) Series P, manufactured by Centerline, Windsor, Canada, was used to coat the stress relieved magnesium alloy samples. In this process, AA7075 powders are accelerated to supersonic velocities by a pressurized nitrogen gas (N_2) through a convergence–divergence de Laval UltiLife TM nozzle. To enable the study of heat transfer in the microstructure evolution of the substrate, we first designed two processing conditions that lead to the manufacturing of two different samples. Table 2 lists the processing parameters for preparing these two different types of samples employed in this study. For both samples, the nozzle standoff distance was kept at 12 mm. However, the first type of samples, called compressive samples herein, was prepared by fixing the substrate on a water-cooled copper plate to facilitate the heat transfer in the substrate. The second type of samples, called tensile samples herein, was prepared using an insulated fixture to prevent the heat transfer in the substrate. Besides controlling the heat transfer in these two samples, the exposure to the heat of the compressive sample was less than the tensile sample. The heat exposure was controlled by the nozzle speed, which was five times faster in the compressive sample. Since all other coating parameters were kept constant, including the feed rate, the thickness of coating in the tensile sample was considerably greater, as reported in the results section. Also, we characterized the samples coated by the processing parameter of Table 2, which

Table 1
Chemical composition of AA7075 coating powders.

Composition	Aluminum (Al)	Zinc (Zn)	Iron (Fe)	Nickel (Ni)	Chromium (Cr)	Copper (Cu)	Magnesium (Mg)	Other Elements
Weight%	90	5.20	0.35	0.005	0.25	1.55	2.35	0.30

Table 2
The processing parameters of cold spray coating for inducing tensile and compressive residual stress in magnesium alloy samples.

Parameters	Tensile samples	Compressive samples
Carrier Gas Temperature (°C)	400	400
Carrier Gas Pressure (psi)	200	200
Speed of Nozzle (mm/s)	2	10
Feed Rate (gr/min)	8	8

has been reported elsewhere [5]. The densities of the samples were measured to be above 99.4% for tensile samples and above 99.9% for compressive ones. The hardness of the AA7075 coating was about 155 HV and 175 HV for tensile and compressive samples, respectively, which are very close to the bulk wrought and cold spray coated AA7075 reported in the literature [15,16].

2.3. Characterization

To evaluate the distribution of residual stresses through the depth of coated samples, a hole drilling machine, Sint technology, Restan MTS-3000, was used to release strain by drilling a small hole in the coating and substrate and measure the relaxation strain and calculate the stress using the non-uniform method [17].

To identify potential phase developments at the interface of coating and substrate the x-Ray diffraction, Bruker D8 Discover, equipped with a Cu-K_α x-Ray tube (40 kV and 40 mA) and VÅNTEC-500 area detector, was employed.

Microstructural analysis was conducted using a high-resolution Keyence optical microscope (VHX6000 manufactured by Keyence Corporation, Osaka, Japan) and SEM (TESCAN VEGA3) for the cross-sectioned cold spray samples. For this, the polished samples were etched using an appropriate etchant, as discussed in [13]. In addition, transmission electron microscopy (TEM, JEOL-2010F) was employed to investigate the interface structure between the coating and substrate. The TEM sample was prepared by the focused ion beam (FIB, Zeiss NVision40), combining a Schottky field emission SEM. The operating voltage of the SEM was 200 KeV. Electron Backscatter Diffraction (EBSD) analysis was performed using a JEOL JSM 7000f SEM with a step size of 0.25–0.55 μm and an accelerating voltage of 20 kV. EBSD data collection was done using Oxford Instruments Aztec software, and post-processing was done using the HKL Channel-5 package [18] and MTEX open source package [19]. For the EBSD sample preparation, the standard procedures followed: mechanical grinding using the SiC papers and diamond polishing to 0.25 μm (1hr) to remove any residual surface deformation and stress from the previous steps. It must be noted that an additional ion-polishing were performed on the prepared EBSD samples to achieve the required surface quality and remove any surface oxide layer.

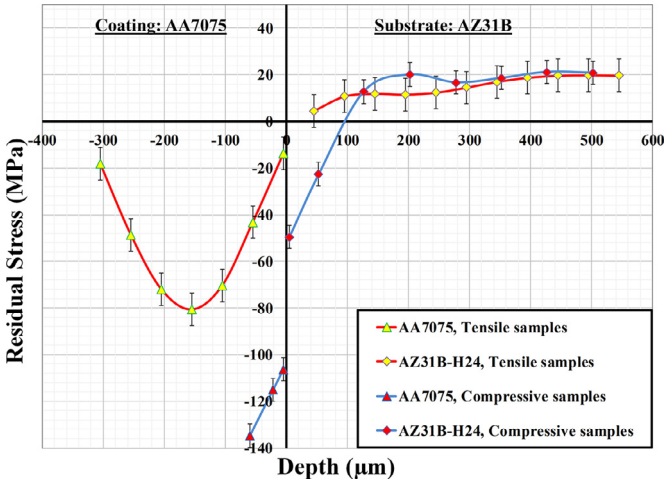

Fig. 2. Residual stress measurements for the two coated samples of this study.

3. Results and discussion

3.1. Customizing residual stress in the substrate

The effect of heat balance in the cold spray process, leading to induced tensile and compressive residual stress, on the microstructural evolution of the substrate was studied. For this, two distinct types of samples with controlled heat transfer were designed and manufactured. To engineer the residual stress in the samples, the reported results by Marzbanrad et al. [5] have been employed. They showed that the underlying parameter in the cold spray process regarding the formation of residual stress in the substrate and coating is the heat balance at the interface region. This includes the heat balance (heat input and heat loss) during the coating process. First, the two types of samples were examined to verify the existence of the tensile and compressive residual stress in the coating and substrate. Fig. 2 shows residual stress distribution for the compressive and tensile samples through the coating thickness and substrates. The residual stresses in these two

samples are distinctly different. The major difference is in the sign of residual stress in the substrate. In tensile samples, the residual stress in the substrate near the interface is positive (tensile), whereas the sign of residual stress at the same location in compressive samples is negative (compressive). In the tensile samples, which have been processed under the lower nozzle speed, higher temperature process and insulated fixture under the substrate, the residual stress of the AA7075 coating is parabolic. Near the coating surface, the residual stress has a lower negative value (about −20 MPa) compared to the middle of the coating thickness, which reaches the maximum level of −80 MPa. It is observed that the residual stress of the interface is about the same value as the coating surface. This trend continues and can even be exacerbated in the temperature-sensitive magnesium substrate. The residual stress distribution depends on the heat transfer between two adjoining materials with different thermal expansion coefficients, which have different thicknesses [5]. Based on the presented results, we were able to successfully engineer the tensile residual stress in the magnesium substrate coated with AA7075. However, by decreasing the thermal energy of the sample, which has been done by increasing the thermal conductivity and using higher nozzle travel speed, we were enabled to develop compressive residual stress of around −50 MPa in magnesium at the interface. It is important to note that decreasing the nozzle speed increases the thickness of the coating, where the coating thickness of the tensile samples (350 μm) was significantly higher than that of the compressive samples (100 μm) with the same step-over of 1.2 mm. By decreasing the nozzle travel speed at a constant feed rate, the number of particles deposited on the substrate as well as the impact temperature is increased, leading to the formation of a thicker coating. It should be considered that the coating thickness reduction has a constructive effect on reducing the mechanical influence of thermal mismatch [5]. It has been demonstrated that recoating the sample can increase the coating thickness while the compressive residual stress is maintained in the substrate [5].

3.2. Phase identification

The net thermal energy accumulation at the interface region, which is a function of the heat input, heat generation upon impact, and heat transfer from this area, may satisfy the thermodynamic requirements for the synthesis of intermetallic phases in the microstructure of the interface region. The formation of intermetallic is important since brittle intermetallic phases can have detrimental influences on the mechanical performance of the interface. Considering the different thermal energy at the interface region of the tensile and compressive samples, the formation of any aluminum-magnesium intermetallic was investigated by XRD characterization. The XRD results are shown in Fig. 3. The XRD patterns of these samples were collected over a more extended period to increase the chance of detecting any phases at the interface. However, analyzing the XRD patterns detected only Al (card number: COD 9,012,428) and $Mg_{0.971}Zn_{0.029}$ (Card Number: COD 1,523,360) for both samples and no difference could be observed in detecting peaks. The development of intermetallic phases, including $Al_{17}Mg_{12}$, has been reported at the interface of aluminum and magnesium when the coated samples were heat-treated at the temperature range from 360 °C to 430 °C for 24 h [20]. In another research, the post-processing was done by annealing at 200 °C for one hour after fabricating Al/Mg/Al laminate by four-pass rolling, and they identified two intermetallic phases of $Mg_{17}Al_{12}$ and Al_3Mg_2 at Mg/Al interface [21]. To the best of our knowledge, only one study has reported the in-situ formation of $Al_{17}Mg_{12}$ during multi-pass cold spray coating. They coated AZ31B with AA7075 under a carrier gas temperature of 400 °C and a pressure of 200 psi, with the nozzle speed of 5 mm/s, and a feed rate of 8 gr/min [22]. However, based on the XRD patterns and in the resolution range of the experiments, no intermetallic phase was found at the interface during coating in this research. Intermetallic phase formation during solidification is a relatively fast process. However, solid-state intermetallic phase formation is a diffusional process and requires: 1) enough thermal energy and 2) ample time for diffusion [23]. Mixing of aluminum and magnesium at the interface is probable during solid-state bonding [22]. Depending on the concentration of this mixture, solid solution or intermetallic phases have a chance to develop at the interface through diffusional mechanisms. However, during cold spray coating, the interface experiences high temperature for a short time, which is a few orders of magnitude less than the time required for diffusion of the atoms. This situation is very far from thermodynamic equilibrium condition. Therefore, as we observed in the XRD patterns, in situ formation of intermetallic phases during the short time of cold spray coating will most likely not occur in the two set of processing parameters, which were customized for the tensile and compressive samples

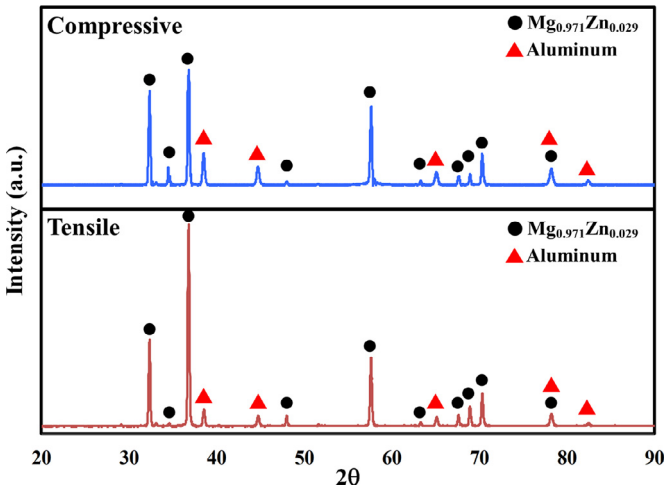

Fig. 3. XRD pattern of the tensile and compressive sample.

3.3. Microstructure of the interface

A transmission electron microscopy (TEM) was performed on the tensile and compressive samples to reveal the grain

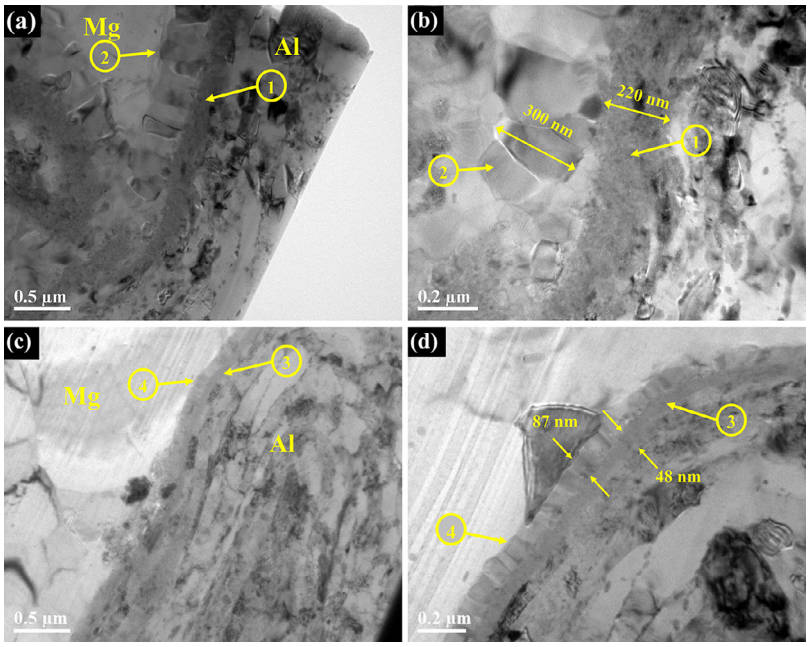

Fig. 4. TEM image of the: a and b) tensile sample; c and d) compressive sample, showing the interface of the coating and substrate including a region of fine grains follows by columnar grains in the magnesium side of the interfaces.

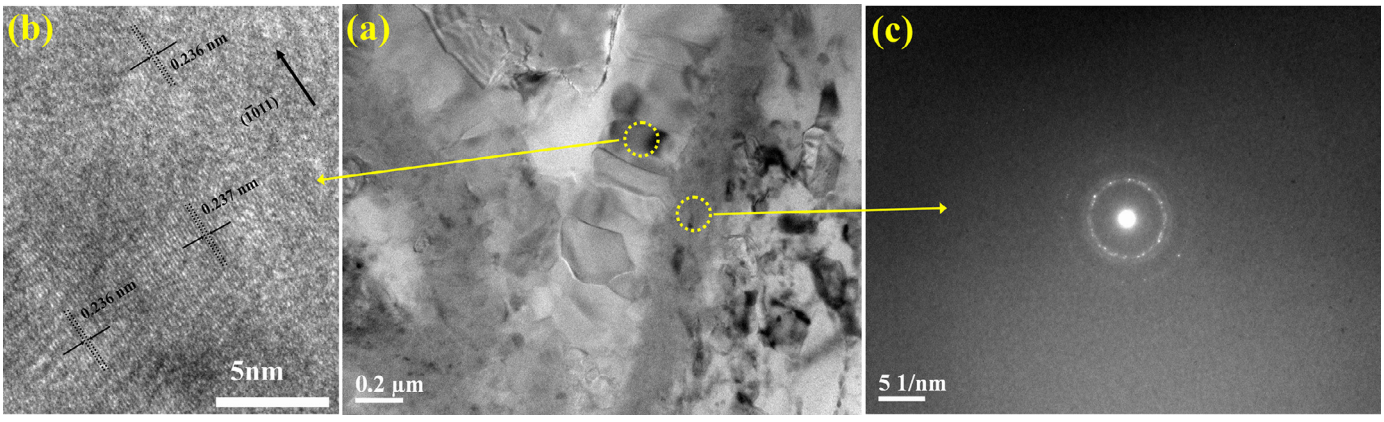

Fig. 5. a) TEM image of the interface; b) high-resolution TEM image of the columnar interfacial grains; c) Selected area diffraction (SAD) pattern of the nanocrystalline grains at the interface region.

structures at the interface and illustrate the role of heat accumulation on the interface microstructure. Fig. 4a and Fig. 4b show the TEM images of the interface for the tensile sample at two different magnifications. Based on the observations, at the interface of the aluminum and the magnesium, a very fine grain zone has been formed, which has been labelled in the image by ①. In the magnesium side of the interface, a ladder shape structure consisting of columnar grains has been developed (marked by ②). TEM images of the compressive sample are shown in Fig. 4c and Fig. 4d with the same magnification of the tensile sample. Based on the TEM images, the grain structures of the interface for compressive samples are similar to the tensile ones. However, the interface features of the compressive sample are smaller than the tensile ones. The fine grain zone of the tensile sample has a thickness of around 220 nm ①, but this zone in the compressive sample is only around 48 nm ③ (Compare Fig. 4b and Fig. 4d). The thickness of the ladder grain region of the tensile sample is also more significant than that of the compressive sample. The columnar grains in the tensile sample are about 300 nm ②, while this size in the compressive sample is only about 87 nm ④. Since the structure of the interface is not changed by altering the coating condition from the tensile to the compressive samples, it may be concluded that the bonding mechanism and the impact effects on both samples are similar. However, the effect of excess thermal energy in the tensile sample can be clearly observed in the size of the interface features.

To identify the structure of the columnar grains, fine grain interfacial zones, and the possibility of formation of intermetallic phases at the interface during bonding, these areas have been studied in detail through high-resolution TEM (HRTEM) and selected area diffraction (SAD) pattern. Fig. 5a shows a TEM image of the interface. Fig. 5b demonstrates an

HRTEM image of these columnar grains. As marked on the image, the distance between the atomic planes of this grain is equal to 0.236 nm, which is close to the interplanar distance of $(\bar{1}011)$ plane of magnesium alloy. This HRTEM image reveals that the ladder shape feature on the magnesium side of the interface consists of the crystalline magnesium grains, which nucleated at the interface and grew perpendicular to the small grain zone interface region, in the direction of heat transfer from the hot interface to the cold substrate. Fig. 5c shows the SAD pattern of the fine-grain interface zone. According to the ring pattern and bright spots on the rings, this area consists of very fine crystalline grains. This feature signifies a highly deformed pattern and a solid-state mixing of the two materials at the interface, formed during particles' impact and the extensive deformation of particles and the substrate surface upon impact. Based on the TEM study, detectible crystal grain of intermetallic phases in the resolution of this TEM study was not formed during coating, which is compatible with the XRD results presented in Fig. 3. The intermetallic phase formation of the fine grains' interface zone is probable, as reported in [22]; however, the HRTEM and SAD patterns do not provide clear evidence for forming the intermetallic phases. More investigation is necessary to confirm the existence of the intermetallic phases in the fine grains interface zone.

3.4. Microstructure of the substrate

Fig. 6a and b show the microstructure of the magnesium alloy substrate near the interface for tensile and compressive samples, respectively, over a wide range of interface and substrate areas. High-magnification SEM images of tensile and compressive samples are depicted in Fig. 7a and b. The optical and SEM images of the tensile sample's microstructure (Fig. 6a and Fig. 7a) show grain refinement formation adjacent to the interface, followed by a region of large grains. Fig. 7c provides a higher magnification picture of one of the large magnesium grains in this region, surrounded by relatively small gains. After this region, the grain size of the magnesium substrate decreases again, as can be observed in Fig. 6a and Fig. 7a. Comparing the microstructure of the compressive sample (see Fig. 6b and Fig. 7b) to that of the tensile sample shows that the grain size of the compressive sample adjacent to the interface (Fig. 7e and f) is smaller than tensile samples. Moreover, Fig. 6b, Fig. 7b and e show that around 25 μm below the interface of the compressive sample, there is a band in which high-intensity twin boundaries are observed inside their grains. Comparing the optical microscopy images of Fig. 6a and b reveals that the accumulation of twin boundaries in the tensile sample happened between 100 μm to 150 μm below the interface. The SEM image of Fig. 7d confirms the existence of twinning in the tensile sample grains at the specified area. It is noted that the dark line observable in Fig. 6a and b between the AA7075 and AZ31B is an artifact of the microscope image due to the different height of the coating and substrate.

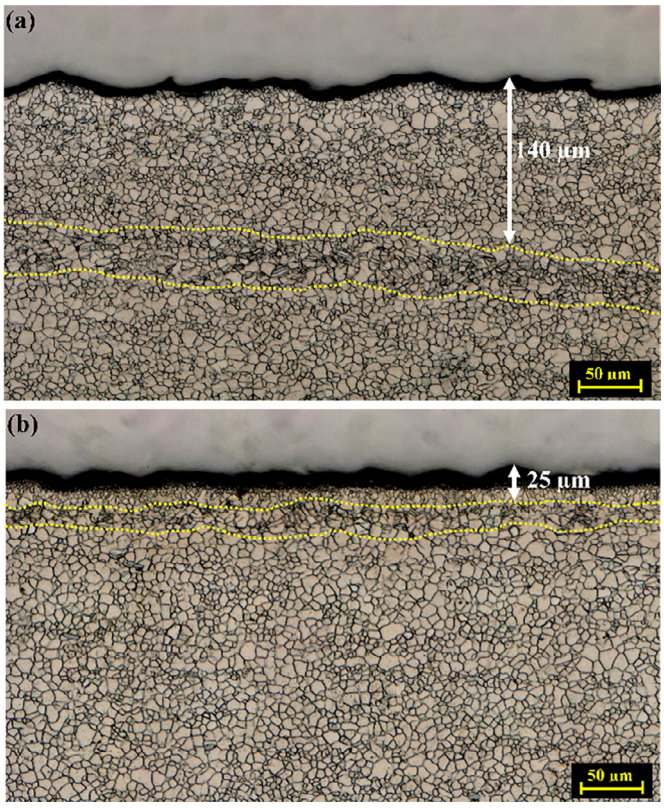

Fig. 6. Microstructure of a) tensile sample; b) compressive sample showing the grain refinement near the interface and the accumulation of twinning in a narrow band parallel to the interface.

The deformation mechanism of AZ31B-H24 magnesium alloy is highly dependent on temperature and strain rate. It is well known that the deformation modes of AZ31B alloy are: basal ⟨a⟩ slip {0001} ⟨1120⟩, prismatic ⟨a⟩ slip {1010} ⟨1120⟩, pyramidal ⟨a⟩ slip {1011} ⟨ 1120⟩, pyramidal ⟨$c+a$⟩ slip {1122} ⟨1123⟩ and tensile twinning mode {1012} ⟨1011⟩ [24–27]. AZ31B alloy sheet has a strong basal texture with a c-axis perpendicular to the surface of the sheet [27,28]. During the cold spray deposition, compressive stress is applied on the top of the surface along the c-axis by particle impact. At low temperatures, a combination of basal slip and tension twinning is necessary for deformation [24,27,29,30]. The critical resolved shear stresses (CRSS) predicted for these mechanisms at different temperatures are listed in Table 3 [31]. These data and other results reported in the literature [32] illustrated that the CRSS of the twinning deformation mechanism increases with increasing temperature, while the CRSS of the other deformation mechanisms such as pyramidal ⟨$c+a$⟩ decreases. Table 3 shows that up to 150 °C, basal slip and twinning have the lowest CRSS compared to other mechanisms; However, at 200 °C, Prismatic slip and pyramidal ⟨$c+a$⟩ have lower CRSS than twinning and, as a consequence, from a specific temperature between 150 °C to 200 °C, the deformation mode changes and the chance for twinning to contribute to the deformation of AZ31B will become very low. Looking at the microstructure of the AZ31B sprayed substrate, Fig. 6a and b, it is apparent that both tensile and

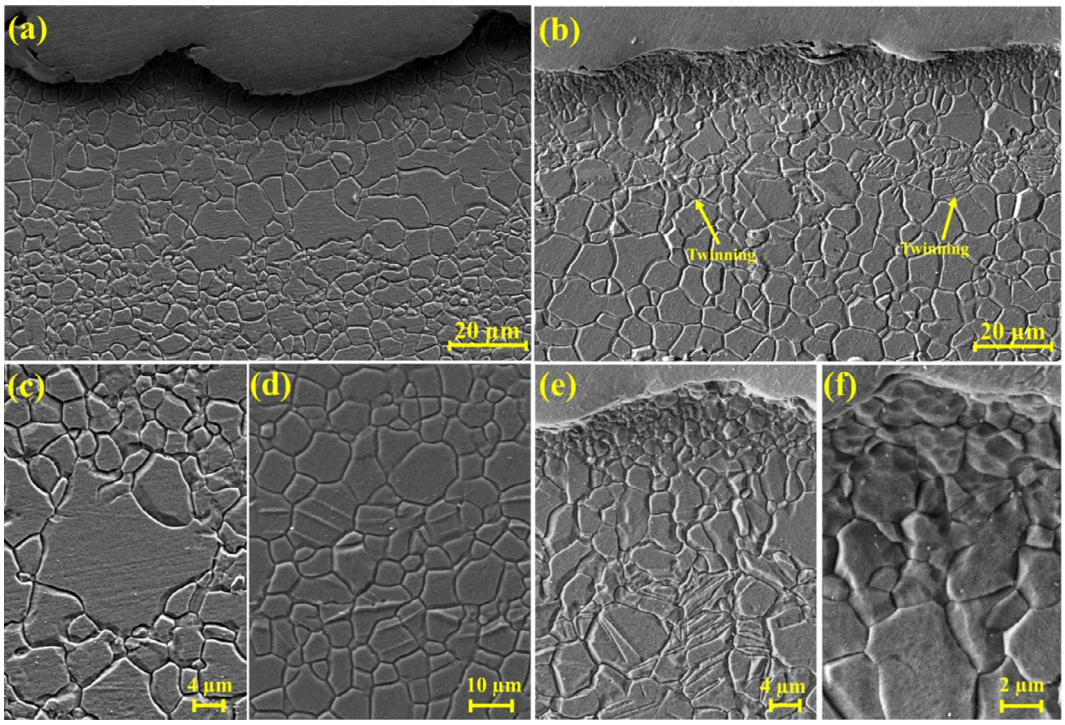

Fig. 7. The SEM images of substrate microstructures: a) tensile sample; b) compressive sample showing the microstructure of the magnesium substrate near the interface; c, d) tensile sample with high resolution showing dynamic grain growth in magnesium substrate and twining in the grains of the twin band region, respectively; e, f) compressive sample with high magnification showing the twin band region of the compressive sample and fine grain structure of magnesium substrate at the interface, respectively.

Table 3
Critical resolve shear stress (CRSS) of different deformation modes for AZ31B at different temperatures [31].

Temperature (°C)	Deformation mode	CRSS (MPa)
100	Basal slip	1.3
	Prismatic slip	75
	Pyramidal $<c+a>$	85
	Tension twin	63
150	Basal slip	1
	Prismatic slip	65
	Pyramidal $<c+a>$	72
	Tension twin	63
200	Basal slip	0.8
	Prismatic slip	44
	Pyramidal $<c+a>$	56
	Tension twin	82

compressive samples have a narrow band parallel to the interface in which the accumulation of twinning can be observed. However, twinning deformation is not seen in the grains between the interface and twin band. These special microstructures represent high temperature deformation of the substrate in the area between the interface and twin band. Comparing the tensile and compressive samples (Fig. 6a and b) demonstrates that the twin band in the tensile sample is around 140 µm from interface, while in the compressive sample, the width of this area is about 25 µm. From this observation, it may be concluded that the high temperature deformation zone in the tensile sample is 5.6 times larger than that of the compressive sample. Since the coating thickness of the tensile samples are more than that of the compressive samples due to the increasing number of particles impact, the substrate of the tensile sample experiences more peening than the compressive samples does. However, the hot deformation area of the tensile samples consists of relatively larger equiaxed grains than are found in the compressive sample (compare Fig. 6a and b). Considering the duration and temperature of the cold spray process, the only explanation for larger equiaxed grains in the tensile samples is dynamic recrystallization and dynamic grain growth processes. The microstructure of the tensile sample shows an abnormal grain growth in the hot deformation region, which is an additional evidence for dynamic grain growth in this condition. Dynamic recrystallization and dynamic grain growth have been reported for AZ31B alloy under a high strain rate and high temperature deformation[29,33–35]. Therefore, the observations of this study seem to be compatible with those in the literature. Comparing the microstructure of the tensile and compressive samples confirms that the proposed strategy for controlling the thermal input (Q1) and heat generation (Q2) during coating and maximizing of the thermal output of the system (Q3) can successfully decrease the temperature of the interface. The temperature optimization process can minimize the dynamic recrystallization and eliminate dynamic grain growth in the compressive samples, providing suitable conditions for improving magnesium's microstructure as well as enhancing its mechanical properties.

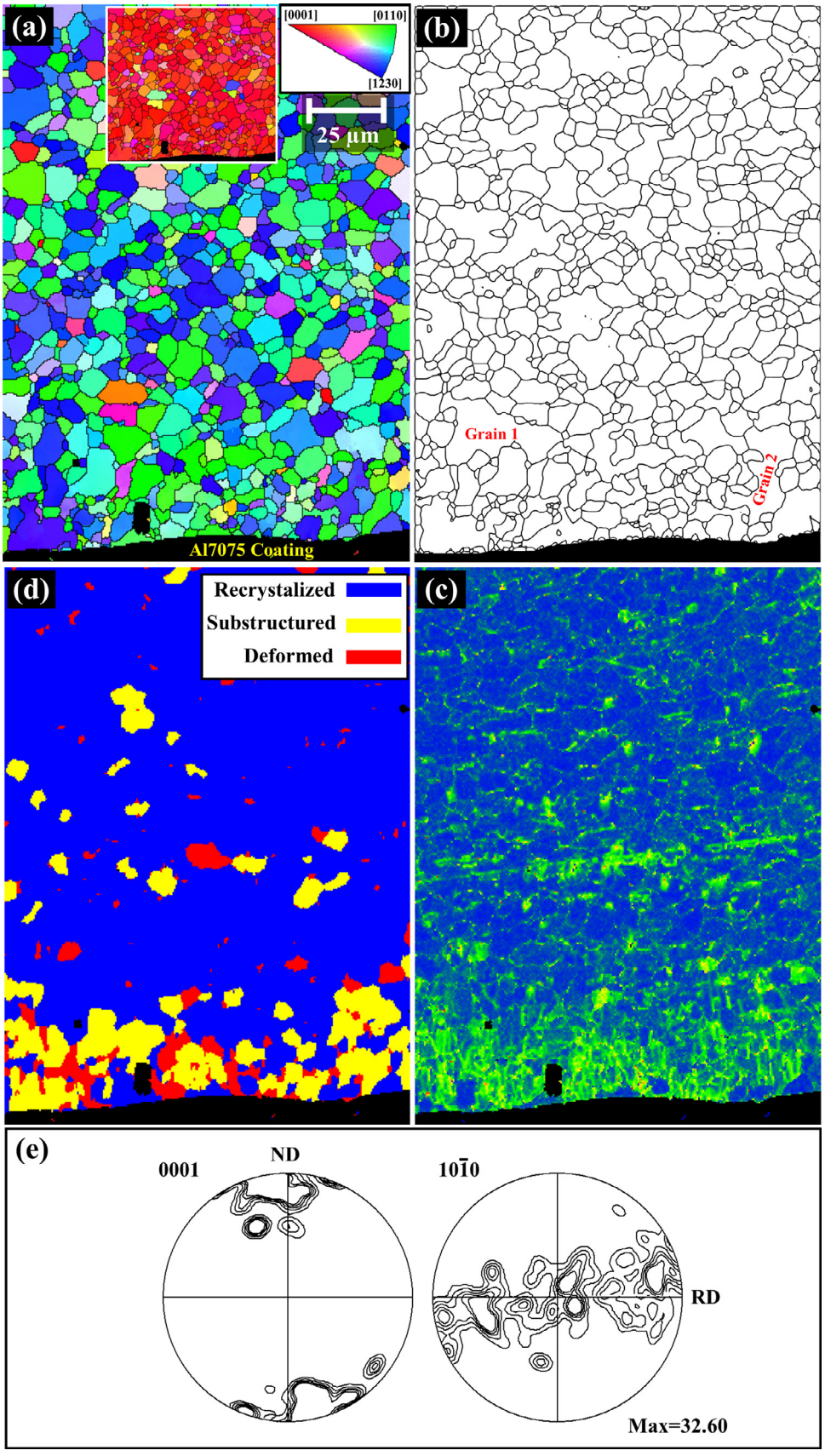

Fig. 8. a) Orientation microscopy imaging (OMI) pattern of the tensile sample; b) Grain boundary structure of the tensile sample close to the interface extracted from EBSD data; c) Kernel average misorientation map (KAM) of the tensile sample close to the interface; d) recrystallization map of the grains in the microstructure of the tensile sample; e) (0001) and (10$\bar{1}$0) pole figures from the interface region (up to 150 µm from the interface).

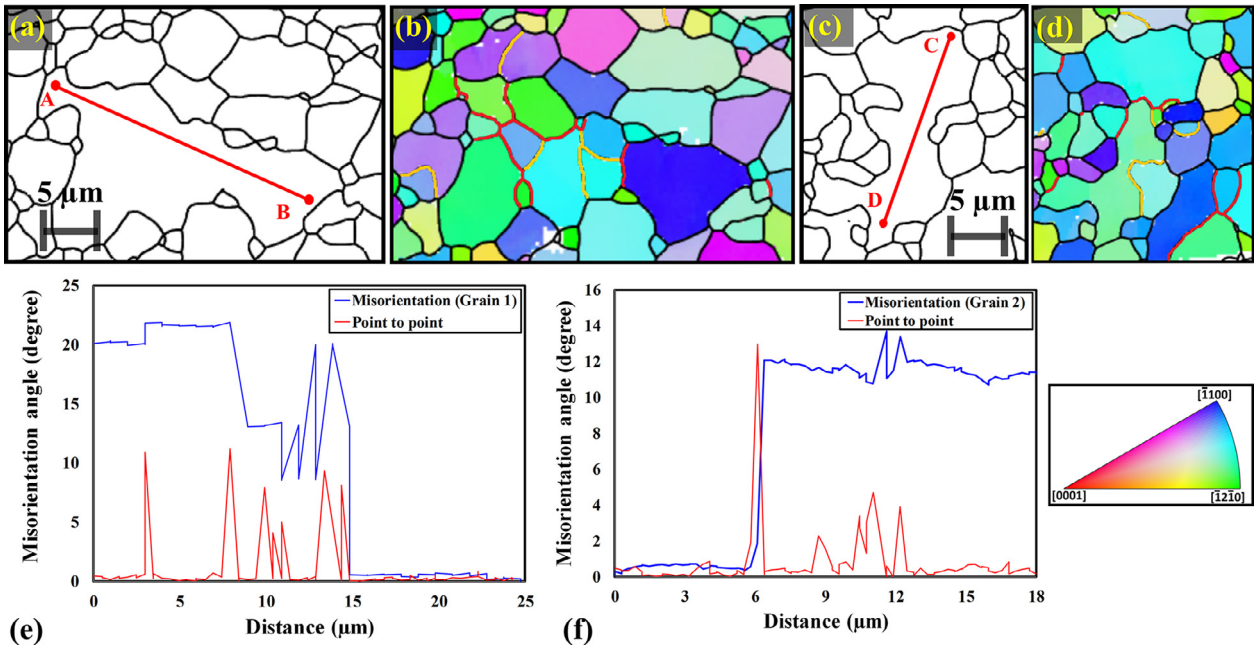

Fig. 9. a and b) Dynamic grain growth close to the interface of the tensile sample and corresponding grain boundary structure and misorientation angle; c and d) Dynamic grain growth close to the interface of the tensile sample and corresponding grain boundary structure and misorientation angle; e) orientation change along line A-B; d) orientation change along line C-D. (Grain boundary colours: yellow <4°, red larger than 4° and smaller than 15°, Black >15°).

3.5. EBSD analysis of the substrate

To further investigate the effect of heat accumulation on the substrate microstructure near the interface of coated samples, the EBSD technique was employed. The goal of the EBSD analysis is to investigate the potential occurrence of thermally activated stress relief, dynamic recrystallization, and dynamic and abnormal grain growth in magnesium substrate. Fig. 8a shows the orientation microscopy imaging (OMI) pattern of quite a large area of magnesium alloy substrate near the interface of the tensile sample. This image shows the random crystallographic texture in the rolling direction (RD), while the inset of Fig. 8a shows the strong [0001] texture in the normal direction (ND). It is noted that the AZ31B sheet has a strong basal texture, which is formed during the rolling process. The recalculated (0001) and ($10\bar{1}0$) complete pole figures within the narrow band of 150 µm below the interface are presented in Fig. 8e. This confirms that the magnesium alloy substrate's strong texture (formed during the rolling process) has not been drastically changed by cold spray deposition. In other words, there is not any extensive grain nucleation and growth with random orientations. The grain boundary map of the scanned area of the tensile sample with a misorientation greater than 15° was extracted from the EBSD data (Fig. 8b). Observed grain size change in Fig. 8a and b agrees with the optical microscopy and SEM micrographs (Fig. 6a and Fig. 7a). The Kernel average misorientation map (KAM) in Fig. 8c shows a high level of misorientation in the sample structure close to the interface. Accumulation of the dislocation in this area represents the deformation and residual stress in this area of the sample. Finally, the grain average misorientation (GAM) method was employed to evaluate the recrystallization of the grains in the microstructure of the tensile sample (Fig. 8d). This map confirms that most affected areas by the cold spray coating (between 100 µm to 150 µm from the interface) and even at some areas adjacent to the interface, the microstructure is recrystallized. In a narrow band of 50 µm from the interface, dislocation pile-up leads to accumulation of low angle grain boundaries, which is evidence for stress relief in this region, although some parts of the substrate adjacent to interface detected as deformed grains confirming elastic strain retention in these grains. The recrystallized grains in the tensile sample support the temperature profile prediction; hence, confirming the suggested deformation mechanism in this cold spray deposition condition.

Microstructural observations of the interface (Fig. 6a and Fig. 7a) also revealed evidence for the dynamic grain growth in the grains close to the interface of the tensile sample. Fig. 9a and c also show representative examples of dynamic grain growth in the region immediately below the surface at the recrystallized region (for example, Grain 1 and Grain 2 in Fig. 8b), while the corresponding misorientation map of these two areas is illustrated in Fig. 9b and d. The misorientation map of these grains (Fig. 9b and d) and local point to point misorientation changes were measured along the line A-B and C-D, showing the low-to-medium lattice orientation transition in the neighbouring interior sub-grains (Fig. 9e and f). This observation shed light on the rapid grain growth mechanism in the region, suggesting dynamic coalescence of the nucleated grains due to the applied heat and stress during the coating process, known as rotation-coupled grain coalescence[36]. It must be noted that the variation of the misorientation angles

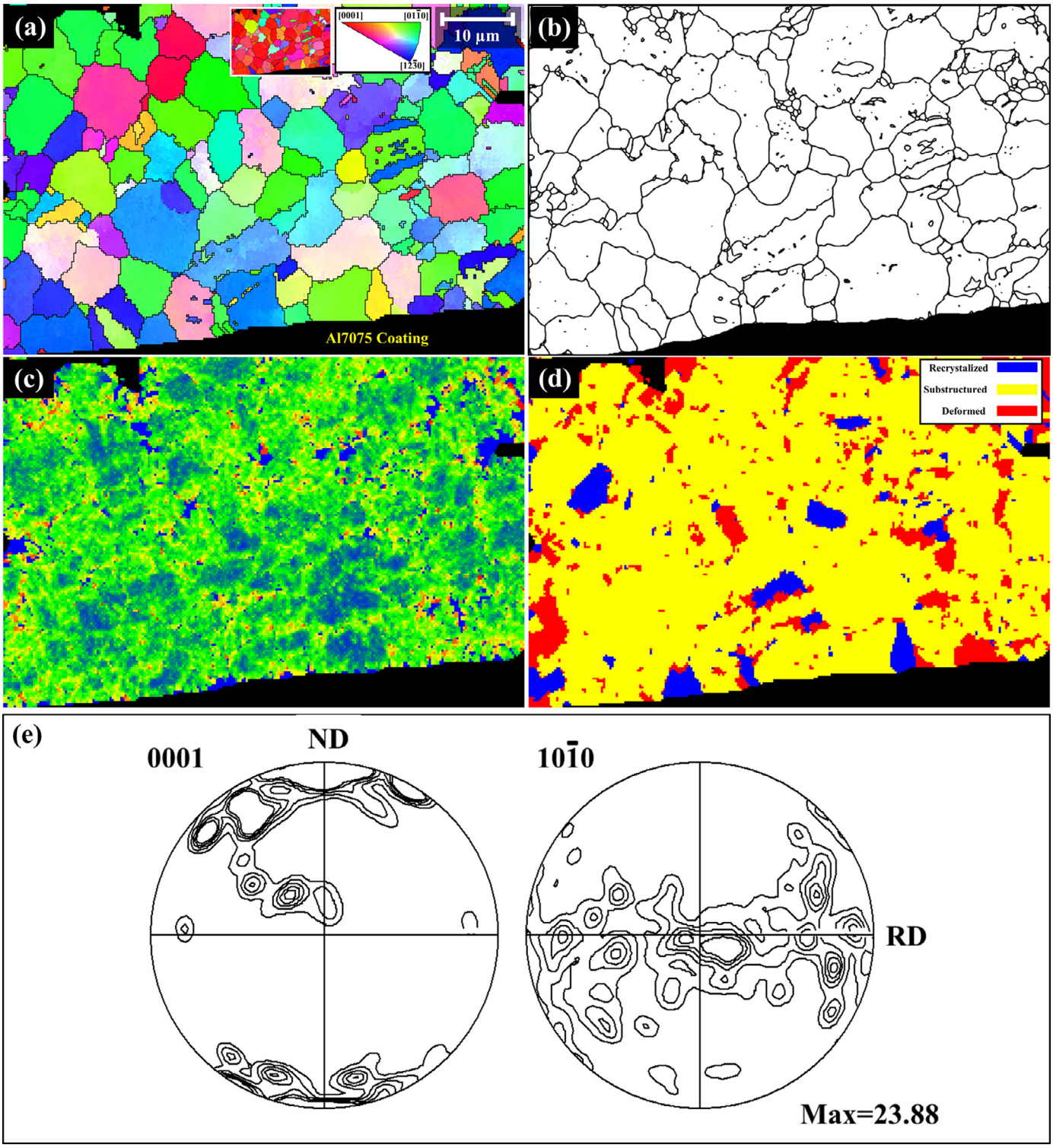

Fig. 10. Orientation microscopy imaging (OMI) pattern of the compressive sample; b) Grain boundary structure of the compressive sample close to interface extracted from EBSD data; c) Kernel average misorientation map (KAM) of the compressive sample close to the interface; d) recrystallization map of the grains in the microstructure of the compressive sample; e) (0001) and (10$\bar{1}$0) pole figures collected from the near interface region.

is in the range of 2–15° due to the different stages of grain coalescence (growth) in the indicated grains of Fig. 9.

Fig. 10a and b show the OMI pattern and grain boundary map of the magnesium substrate for the compressive sample. Comparing Fig. 10a and b with Fig. 8a and b shows that the grain size of the affected area of the compressive sample substrate is much smaller than the tensile sample, which is in line with the optical microscopy and SEM observations (Fig. 6 and

Fig. 7). Moreover, coalescence and dynamic grain growth are not observed in the compressive sample, confirming the other microstructural observations of this research. The KAM map of the scanned area (Fig. 10c) shows high dislocation density, and the grain average misorientation (GAM) of the compressive sample (Fig. 10d) revealed the accumulation of substructures grains in this area. The small number of recrystallized grains and the presence of deformed grains in the substrate of the compressive sample adjacent to the interface along with the accumulation of dislocation in the area is presented by the KAM map, confirms the effect of lower temperature on the microstructure during this cold spray condition, which induced the beneficial residual stress in the substrate after coating. The recalculated (0001) and $(10\bar{1}0)$ complete pole figures from the near interface area are presented in Fig. 10e. Comparing the pole figures of Fig. 8e and Fig. 10e (the tensile and compressive samples) shows a greater extent of weakening of the material's initial basal texture in the compressive sample (the effect of deformation of the grains and residual stress in the compressive sample).

4. Conclusion

The structure of the interface and substrate next to the interface have been studied to clarify the effects of heat balance on the microstructural evolution and residual stress development of AZ31B substrate coated with AA7075 alloy through the cold spray process. For this study, two sets of high and low thermal energy coating conditions were designed for the deposition. The residual stress of the coating and substrate were measured for these two samples. Tensile and compressive residual stresses were induced under high and low thermal energy of the system, respectively. The following conclusions can be drawn from the results:

1) The phase identifications of the tensile and compressive samples showed no signs of the intermetallic phase being developed by the coating process at the interface of the samples. The heat accumulation in the interface region of the tensile and compressive sample was not enough to provide the chance of intermetallic phase growth in this region.
2) TEM microscopy confirmed that for both high and low thermal energy coating conditions, a fine grain region followed by a columnar grain on magnesium substrate were formed, which grew perpendicular to the fine grain zone in the magnesium side of the interface. Low thermal energy leads to a 78% thinner fine grains interfacial area and 71% smaller columnar grains.
3) The selected area diffraction pattern of the fine-grain interfacial zone illustrates that this area of the interface consists of fine crystalline embryos, but no significant intermetallic phase development could be detected in this region. Moreover, a high-resolution TEM study of the columnar grains confirmed that these grains are magnesium, and no other phases developed in this area.
4) Optical microscopy, SEM study, and EBSD analysis of the magnesium substrate near the interface showed that equiaxed grains were formed near the interface by dynamic recrystallization. High thermal energy coating of the tensile sample leads to a higher temperature at the substrate near the interface. In this situation, not only dynamic recrystallization but also dynamic grain growth is observed in the substrate near the interface (the size of the grown grains in this region is above 10 μm). Decreasing the temperature resulted in smaller grains ($\leq$ 1 μm) being observed in the compressive sample due to the predominant peening effect.
5) Heat accumulation in the tensile sample during coating leads to dynamic coalescence of the nucleated grains process, known as rotation-coupled grain coalescence.
6) The accumulation of twins in a band parallel to the interface was observed in both tensile and compressive samples. Twinning is an indispensable part of the low-temperature deformation mechanism for magnesium under this loading condition. Therefore, the existence of the twin band was considered as evidence for the substrate temperature at this region. The higher thermal energy of the coating leads to the formation of the twin band away from the interface and in an area around 140 μm from the interface. However, decreasing the heat input pushes the twin band around 82% toward the interface, making the interface temperature in the compressive sample less than that of the tensile sample and inducing compressive residual stress in the former.

Acknowledgement

The financial support of the Natural Sciences and Engineering Research Council of Canada (NSERC) through the Automotive Partnership Canada (APC) under APCPJ 459269–13 grant with contributions from Multimatic Technical centre, Ford Motor Company, and Centerline Windsor are acknowledged. Funds from NSERC-RTI program under EQPEQ458441–2014 grant also supported this research.

References

[1] S. Ehrenberger, Assessment of magnesium components in vehicle, 2013.
[2] M. Gupta, N.M.L. Sharon, Magnesium, magnesium alloys, and magnesium composites, Wiley, 2011.
[3] Y.K. Wei, X.T. Luo, Y. Ge, X. Chu, G.S. Huang, C.J. Li, Deposition of fully dense Al-based coatings via in-situ micro-forging assisted cold spray for excellent corrosion protection of AZ31B magnesium alloy, J Alloys Compd 806 (2019) 1116–1126, doi:10.1016/j.jallcom.2019.07.279.
[4] S.B. Dayani, S.K. Shaha, R. Ghelichi, J.F. Wang, H. Jahed, The impact of AA7075 cold spray coating on the fatigue life of AZ31B cast alloy, Surf Coatings Technol 337 (2018) 150–158, doi:10.1016/j.surfcoat.2018.01.008.
[5] B. Marzbanrad, E. Toyserkani, H. Jahed, Customization of residual stress induced in cold spray printing, J Mater Process Technol 289 (2021) 116928, doi:10.1016/j.jmatprotec.2020.116928.
[6] P. Cavaliere, Cold-spray coatings recent trends and future perspectives, Springer Nature, Switzerland, 2018.
[7] A. Papyrin, V. Kosarev, S. Klinkov, A. Alkhimov, V. Fomin, Cold spray technology, 1st ed., Elsivier, Amsterdam, 2006.

[8] Y.K. Wei, X.T. Luo, X. Chu, G.S. Huang, C.J. Li, Solid-state additive manufacturing high performance aluminum alloy 6061 enabled by an in-situ micro-forging assisted cold spray, Mater Sci Eng A 776 (2020) 139024, doi:10.1016/j.msea.2020.139024.

[9] W. Liu, G. Wu, C. Zhai, W. Ding, A.M. Korsunsky, Grain refinement and fatigue strengthening mechanisms in as-extruded Mg-6Zn-0.5Zr and Mg-10Gd-3Y-0.5Zr magnesium alloys by shot peening, Int J Plast 49 (2013) 16–35, doi:10.1016/j.ijplas.2013.02.015.

[10] G. Shayegan, H. Mahmoudi, R. Ghelichi, J. Villafuerte, J. Wang, M. Guagliano, H. Jahed, Residual stress induced by cold spray coating of magnesium AZ31B extrusion, Mater Des 60 (2014) 72–84, doi:10.1016/j.matdes.2014.03.054.

[11] X.T. Luo, C.X. Li, F.L. Shang, G.J. Yang, Y.Y. Wang, C.J. Li, High velocity impact induced microstructure evolution during deposition of cold spray coatings: a review, Surf Coatings Technol 254 (2014) 11–20, doi:10.1016/j.surfcoat.2014.06.006.

[12] H. Jahed, R. GhelichiJ. Villafuerte (Ed.), Residual stresses and fatigue life enhancement of cold spray, Mod. cold spray mater. process. appl. (2015) 225–252, doi:10.1007/978-3-319-16772-5_5.

[13] B. Marzbanrad, H. Jahed, E. Toyserkani, On the evolution of substrate's residual stress during cold spray process: a parametric study, Mater Des 138 (2018) 90–102, doi:10.1016/j.matdes.2017.10.062.

[14] Metal handbook: 4E: heat treating of nonferrous alloys, ASM International, 2018.

[15] M.R. Rokni, C.A. Widener, G.A. Crawford, M.K. West, An investigation into microstructure and mechanical properties of cold sprayed 7075 Al deposition, Mater Sci Eng A. 625 (2015) 19–27, doi:10.1016/j.msea.2014.11.059.

[16] A. Sabard, P. McNutt, H. Begg, T. Hussain, Cold spray deposition of solution heat treated, artificially aged and naturally aged Al 7075 powder, Surf Coatings Technol 385 (2020) 125367, doi:10.1016/j.surfcoat.2020.125367.

[17] G.S. Schajer, Measurement of non-uniform residual stresses using the hole-drilling method. part i—Stress calculation procedures, J Eng Mater Technol 110 (1988) 338–343.

[18] F. Bachmann, R. Hielscher, H. Schaeben, Grain detection from 2d and 3d EBSD data-Specification of the MTEX algorithm, Ultramicroscopy 111 (2011) 1720–1733, doi:10.1016/j.ultramic.2011.08.002.

[19] F. Bachmann, R. Hielscher, H. Schaeben, Texture analysis with MTEX-free and open source software toolbox, Solid State Phenom 160 (2010) 63–68, doi:10.4028/www.scientific.net/SSP.160.63.

[20] M.X. Zhang, H. Huang, K. Spencer, Y.N. Shi, Nanomechanics of Mg-Al intermetallic compounds, Surf Coatings Technol 204 (2010) 2118–2122, doi:10.1016/j.surfcoat.2009.11.031.

[21] H. Nie, W. Liang, H. Chen, F. Wang, T. Li, C. Chi, X. rong Li, A coupled EBSD/TEM study on the interfacial structure of Al/Mg/Al laminates, J Alloys Compd 781 (2019) 696–701, doi:10.1016/J.JALLCOM.2018.11.366.

[22] S.K. Shaha, H. Jahed, Characterization of nanolayer intermetallics formed in cold sprayed Al powder on Mg substrate, Materials (Basel) 12 (2019), doi:10.3390/ma12081317.

[23] H. Mehmer, Diffusion in solids, Springer, 2010, pp. 784–789, doi:10.1109/IROS.2010.5652268.

[24] S.R. Agnew, O. Duygulu, Plastic anisotropy and the role of non-basal slip in magnesium alloy AZ31B, Int J Plast 21 (2005) 1161–1193.

[25] J. Koike, Enhanced deformation mechanisms by anisotropic plasticity in polycrystalline Mg alloys at room temperature, Metall Mater Trans A Phys Metall Mater Sci 36 (2005) 1689–1696, doi:10.1007/s11661-005-0032-4.

[26] H. Li, E. Hsu, J. Szpunar, H. Utsunomiya, T. Sakai, Deformation mechanism and texture and microstructure evolution during high-speed rolling of AZ31B Mg sheets, J Mater Sci 43 (2008) 7148–7156, doi:10.1007/s10853-008-3021-3.

[27] Y.N. Wamg, J.C. Huang, Texture analysis in hexagonal material, Mater Chem Phys 81 (2003) 11–26.

[28] X.Y. Lou, M. Li, R.K. Boger, S.R. Agnew, R.H. Wagoner, Hardening evolution of AZ31B Mg sheet, Int J Plast 23 (2007) 44–86.

[29] J.A. Del Valle, M.T. Pérez-Prado, O.A. Ruano, Deformation mechanisms responsible for the high ductility in a Mg AZ31 alloy analyzed by electron backscattered diffraction, Metall Mater Trans A Phys Metall Mater Sci 36 (2005) 1427–1438, doi:10.1007/s11661-005-0235-8.

[30] Y.N. Wang, J.C. Huang, The role of twinning and untwinning in yielding behavior in hot-extruded Mg-Al-Zn alloy, Acta Mater 55 (2007) 897–905, doi:10.1016/j.actamat.2006.09.010.

[31] G. Zhou, M.K. Jain, P. Wu, Y. Shao, D. Li, Y. Peng, Experiment and crystal plasticity analysis on plastic deformation of AZ31B Mg alloy sheet under intermediate temperatures: how deformation mechanisms evolve, Int J Plast 79 (2016) 19–47, doi:10.1016/j.ijplas.2015.12.006.

[32] A. Khosravani, J. Scott, M.P. Miles, D. Fullwood, B.L. Adams, R.K. Mishra, Twining in magnesium alloy AZ31B under different paths at moderatly elevated temperature, Int J Plast 45 (2013) 160–173.

[33] Q. Yang, A.K. Ghosh, Formability of ultrafine-grain Mg Alloy AZ31B at warm temperatures, Metall Mater Trans A Phys Metall Mater Sci 39 (2008) 2781–2796, doi:10.1007/s11661-008-9551-0.

[34] I. Ulacia, N.V. Dudamell, F. Gálvez, S. Yi, M.T. Pérez-Prado, I. Hurtado, Mechanical behavior and microstructural evolution of a Mg AZ31 sheet at dynamic strain rates, Acta Mater 58 (2010) 2988–2998, doi:10.1016/j.actamat.2010.01.029.

[35] X. Yang, H. Miura, T. Sakai, Dynamic nucleation of new grains in magnesium alloy during hot deformation, Mater Sci Forum 419–422 (2003) 515–520, doi:10.4028/www.scientific.net/msf.419-422.515.

[36] H. Masuda, T. Kanazawa, H. Tobe, E. Sato, Dynamic anisotropic grain growth during superplasticity in Al–Mg–Mn alloy, Scr Mater 149 (2018) 84–87, doi:10.1016/j.scriptamat.2018.02.021.